ICIC Express Letters
Part B: Applications
Volume **11**, Number **3**, March **2020**

ICIC International ©2020 ISSN 2185-2766
pp. **213–220**

A NEW DAMAGE INDICATOR FOR STRUCTURAL HEALTH MONITORING: EULER-BERNOULLI BEAM CASE

Fergyanto Efendy Gunawan

Industrial Engineering Department, BINUS Graduate Program – Master of Industrial Engineering
Bina Nusantara University
Jl. K. H. Syahdan No. 9, Kemanggisan, Palmerah, Jakarta 11480, Indonesia
fgunawan@binus.edu

Received September 2019; accepted December 2019

Abstract. *With the adoption of damage tolerance design principle, the health monitoring system has become an integral part of the engineering structure in operation. For the system to work, damage indicator that describes the structural integrity level should be established and monitored. Damage indicator is usually derived from structural responses. Many quantities have been proposed for damage indicator. Some popular damage indicators are natural frequency, mode shape, curvature, strain energy, and t-, F-, and z-statistics. In this paper, we propose a new damage indicator derived from the theory of the strength of materials. We evaluate the proposal for a case involving damage on a simply-supported beam. The required data are established numerically by the finite element method for structure in healthy and damaged conditions. The results suggest that the current proposal is more sensitive to damage than the natural frequency.*

Keywords: Structural health monitoring, Damage indicator, Natural frequency, Finite element method

1. **Introduction.** During the last thirty years, the number of research papers about Structural Health Monitoring (SHM) increases tremendously. Those papers reported the applications of SHM on various engineering structures, such as aircraft [1–4] and bridge [5–11]. Meanwhile, the number of articles about machine learning also grows at a massive rate. Machine learning has been used to solve various engineering problems, including for SHM [2, 3, 12–19]. A few journals such as *Mechanical Systems and Signal Processing* and *Journal of Sound and Vibration* put forward the remarks regarding the trend. They consider that applying machine learning only to solving mechanical system problems without applying sound engineering principles is insufficient to justify publication.

In the field of SHM, one major issue is finding indicators that are sensitive to damages. They should easily be measured. So far, many indicators have been proposed. Two popular ones are natural frequency and mode shape [9, 20–25]. The others are vibration curvature [26–28], elastic energy [29], and the power spectral density [30].

Those indicators are useful despite their limitations. Natural frequency and mode shape are good indicators. Natural frequency is global as damage at any point on a structure affects the indicator. However, when damage happens, natural frequency often only changes slightly to be detectable. Mode shape is also global, but the measurement at several points is required to establish the indicator. Vibration curvature and elastic energy possess similar characteristics. The power spectral density can hardly differentiate the healthy condition from the damaged condition when the damage level is small as pointed out by [30].

A new and better indicator is required. It should be more sensitive to damage, require a minimum amount of data, and be easily measured. This paper addresses the issue. It

DOI: 10.24507/icicelb.11.03.213

proposes an indicator developed based on our understanding of the theory regarding the strength of materials. An initial assessment of the method applied to a spring-mass system is presented in [31]. In the previous work, the approach was evaluated on an idealized system where engineering structure was regarded as a system of the concentrated massed connected by elastic springs. We understand that engineering structures are far more complex. Despite the fact, engineers often consider a complex engineering structure as constructed from four basic structures, namely, bar, beam, membrane, and shell. In this work, we evaluate our proposal on a beam structure, a widely used basic structure.

We structure the paper as the following. Section 2, describes the derivation of the damage indicator and the method to generate sample data where the indicator is empirically evaluated. Section 3, presents the results of the computed damage indicator. In this section, we also compare with the results of natural frequency method. Finally, in Section 4, we conclude the most essential aspects contributed by this research.

2. **Research Method.** This paper proposes a damage indicator derived from the theory of the strength of materials. Notably, it focuses on the Euler-Bernoulli beam theory. Thus, the derived indicator is useful for the SHM of beam-like structures.

The Euler-Bernoulli beam theory is accurate when the beam deflection is small such that the beam cross-section remains flat upon deformation. Also, the section is still perpendicular to the beam neutral plane.

With those assumptions, the theory links the applied distributed loads onto the beam $q(x)$ to deformation $w(t, x)$ with the second-order differential equation of [32]

$$EI\frac{\partial^4 w}{\partial x^4} = -\rho\frac{\partial^2 w}{\partial t^2} + q(x). \tag{1}$$

The symbol E denotes the beam elastic modulus, I denotes the second moment of area of the beam cross-section, and ρ is the material density.

The dynamic equilibrium equation is applicable for any point at the beam at any time. We hypothesize that a deviation from the condition may signify a change in either the material properties or the beam geometry or both. Corrosion or crack may alter beam cross-section. Thus, the change may reflect the deterioration in material integrity.

In this work, we use the Euler-Bernoully theory not to predict a beam deformation, nor to predict the exerted force, but to estimate the beam integrity. For the purpose, we propose:

$$d(x, t) = \left| EI\frac{\partial^4 w}{\partial x^4} + \rho\frac{\partial^2 w}{\partial t^2} - q(x)\right|. \tag{2}$$

We hypothesize when the beam is intact, and E, I, and ρ are assigned with values on the intact condition, the damage indicator $d(t, x)$ should be zero or very small. The indicator may shift from zero when the beam contains damages. We assume that damages alter the beam deformation $w(t, x)$.

For SHM purpose, we have the freedom to choose the observation or measurement point. We may select the point where the external load is absent. Thus, it simplifies the computation of the damage indicator.

In this paper, we evaluate the above proposed indicator with a case of damage on a simply-supported beam. The beam has 300-mm length, 20-mm width, and 20-mm height. The beam and its discretization are shown in Figure 1. It is made of steel material with the elastic modulus of 207 GPa, the Poisson ratio of 0.3, and the material density of 8050×10^{-9} kg/mm^3. The beam is subjected to a harmonic load $f(t) = 100 \cdot \sin(2\pi f_p t)$ at the location $x = 100$ mm with $f_p = 2$ kHz.

We compute the beam displacement using Ansys, a commercial finite element package. For the purpose, we discretize the beam with 100 beam elements. Each is 3-mm length.

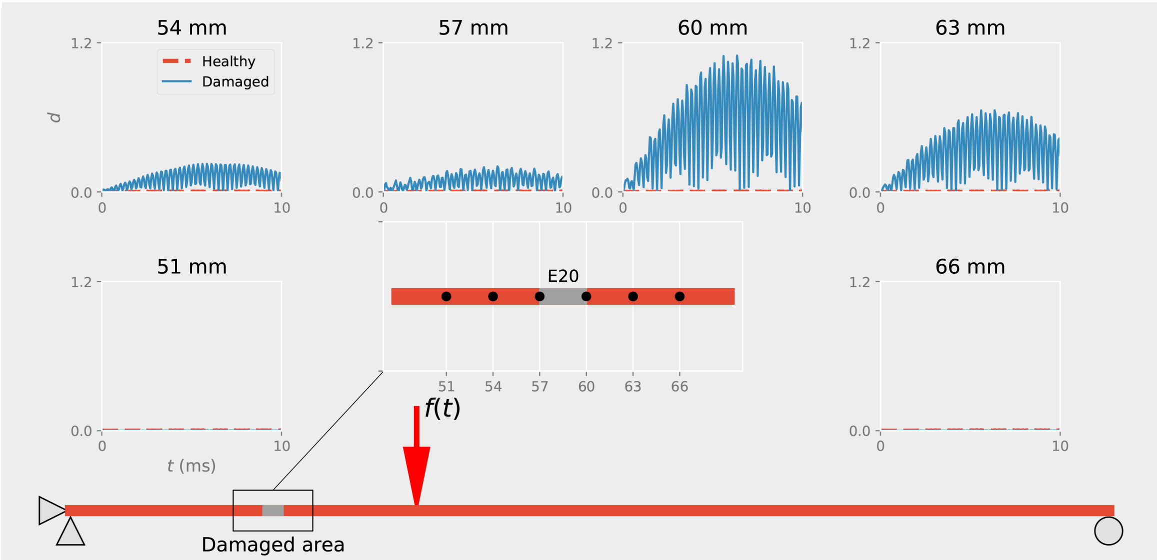

Figure 1. The indicator d computed at the observation points located at 51 mm, 54 mm, 57 mm, 60 mm, 63 mm, and 66 mm for the healthy and damaged conditions. The damaged element, marked by 'E20', spans between $x = 57$ mm and $x = 60$ mm. The duration of analysis is 10 ms.

We have to establish $w(t, x)$ for intact condition as well as damaged condition. For the latter, we assume the damage exists only in Element 20, marked as 'E20' in Figure 1. The element connects the nodes located at x-axis of 57 mm and 60 mm. We also assume the damage reduces the beam elastic modulus as much as five percent.

To compute the damage index $d(t, x)$ by Equation (2), we should establish the terms: $\partial^4 w/\partial x^4$ and $\partial^2 w/\partial t^2$. In the following, we discuss our approach to establish the two terms.

We compute the term $\partial^4 w/\partial x^4$ by the finite difference approximation of:

$$\frac{\partial^4 w(x,t)}{\partial x^4} \approx \frac{w(x-2h,t) - 4w(x-h,t) + 6w(x,t) - 4w(x+h,t) + w(x+2h,t)}{h^4}, \tag{3}$$

where h is taken as the element length of 3 mm.

As for the term $\partial^2 w/\partial t^2$, we firstly fit the displacement time-history data with a cubic spline function and then take the first and the second derivatives of the function to provide the acceleration. The derivation of the cubic spline function is as the following.

We consider n data points: $[(t_1, s(t_1)), (t_2, s(t_2)), \ldots, (t_n, s(t_n))]$. Strictly, we have the condition: $t_1 < t_2 < \cdots < t_n$. We fit the segment in $[t_j, t_{j+1}]$ with a third order polynomial where j is an index from 1 up to n. The polynomial can be written in the Newton form as:

$$p_j(t) = c_{1,j} + c_{2,j}(t - t_j) + c_{3,j}(t - t_j)^2 + c_{4,j}(t - t_j)^3. \tag{4}$$

To complete the polynomial, we should determine the values of the four coefficients: $c_{1,j}$, $c_{2,j}$, $c_{3,j}$, and $c_{4,j}$. They can be computed by:

$$c_{1,j} = s(t_j), \tag{5}$$

$$c_{2,j} = m_j, \tag{6}$$

$$c_{3,j} = \frac{[t_j, t_{j+1}]s - m_j}{\Delta t_j} - c_{4,j}\Delta t_j \quad \text{and} \tag{7}$$

$$c_{4,j} = \frac{m_j + m_{j+1} - 2[t_j, t_{j+1}]s}{(\Delta t_j)^2}. \tag{8}$$

The term m_j denotes the gradient at point t_j. The terms $[t_i, \ldots, t_{i+k}]s$ denotes the kth divided difference of s at the points $t_1, \ldots, t_{i+k}$. It can be computed by:

$$[t_i, \ldots, t_{i+r}]s = \frac{[t_{i+1}, \ldots, t_{i+r}]s - [t_i, \ldots, t_{i+r-1}]s}{t_{i+1} - t_i}.$$

For given the slopes m_1 at the first point t_1 and m_n at the last point t_n, we can compute the gradients at the points $t_2, t_3, \ldots, t_{n-1}$ by solving a set of linear equations:

$$\Delta t_j \cdot m_{j-1} + 2(\Delta t_{j-1} + \Delta t_j) \cdot m_j + \Delta t_{j-1} \cdot m_{j+1} = 3\left(\Delta t_j [t_{j-1}, t_j]s + \Delta t_{j-1}[t_j, t_{j+1}]s\right), \quad (9)$$

leading to the gradients $m_2, m_3, \ldots, m_{n-1}$. With these results, we establish the cubic splines for interpolation of the data $w(x, t)$ across the time domain.

3. **Results and Discussion.** In this paper, we propose the formula in Equation (2) for SHM. Our early work suggested the formula was able to detect damage when the measurement was performed near the location of damage [31]. It was evaluated on simple cases involving lumped-mass systems. In this paper, we evaluate the theory for detecting the damages in a beam.

For the reason, we focus on the six measurement points depicted in Figure 1. The points position around the damage. The damage spans the segment between $x = 57$ mm and $x = 60$ mm. The six points are located at $x = 51$ mm, 54 mm, …, 66 mm. Thus, two points are at the ends of the damaged segment, two points on the left of the damaged element, and two points on the right.

We structure this section as follows. First, we present the displacement at those observation points for healthy and damaged conditions. Second, we present the natural frequency for both conditions. Third, we show the proposed damage indicator computed on those observation points. Finally, we present the proposed indicator in the frequency domain.

For the first result, the beam displacements in the lateral direction at the six measurement points are shown in Figure 2 for healthy and damaged conditions. The profiles look rather similar because the six measurement points are separated by the small distance of 3 mm only. It is interesting to witness that the profiles for healthy and damaged conditions look rather identical. The displacements are practically not affected by the five-percent stiffness degradation on Element 20. The fact suggests the quantity is not suitable for damage detection.

For the second result, we focus on the natural frequency. The quantity is computed by solving $\det(\mathbf{K} - \omega^2\mathbf{M}) = 0$, where $\mathbf{K}$ is the stiffness matrix, $\mathbf{M}$ is the mass matrix, and ω is the natural frequency. The computed natural frequency is precise. The approach avoids errors that may occur when the quantity is reduced from the frequency analysis.

The computed natural frequency is shown in Table 1. Only the first nine modes are provided. The table presents the quantity for healthy and damaged conditions. On the last column, the change of the frequency due to the damage is provided. The results suggest that the change of the natural frequency is too small. The damage does not lead to a significant change in the natural frequency.

The natural frequency is well known to be sensitive to damage. Theoretically, damage at any point at the beam should affect the quantity. With this nature, the indicator is said to be global in detecting damage. However, for the present case, it becomes apparent that sufficiently large damage is required to be detectable by the approach. As the natural frequency is proportional to the square root of the stiffness, a 75-percent reduction in the stiffness only changes the natural frequency by half.

For the third result, we present the current proposal of the damage indicator. We compute the indicator at the six observation points. The results are shown in Figure 1. We observe the indicator closely and obtain the following conclusions. The values of the indicator computed at the six observation points are always zero for the healthy condition.

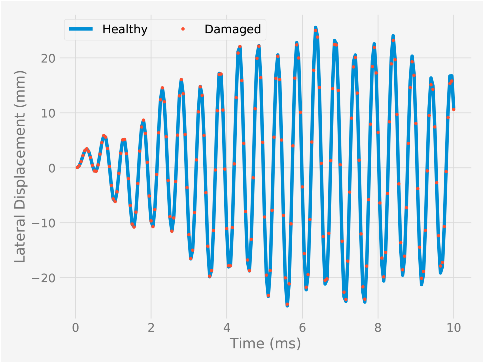

(a) $x = 51$ mm

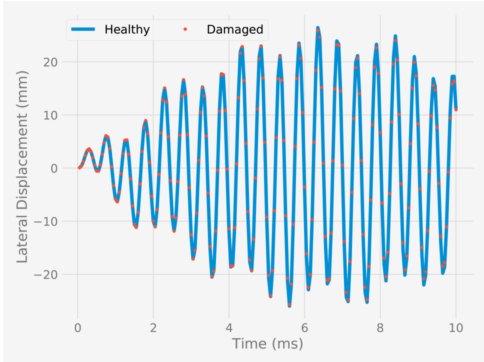

(b) $x = 54$ mm

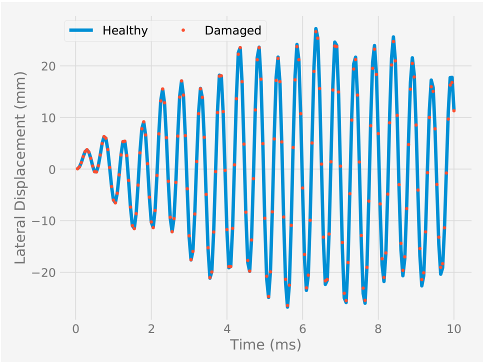

(c) $x = 57$ mm

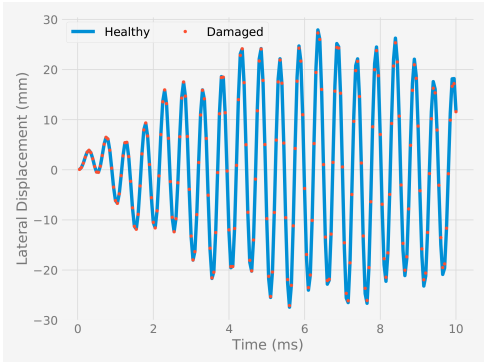

(d) $x = 60$ mm

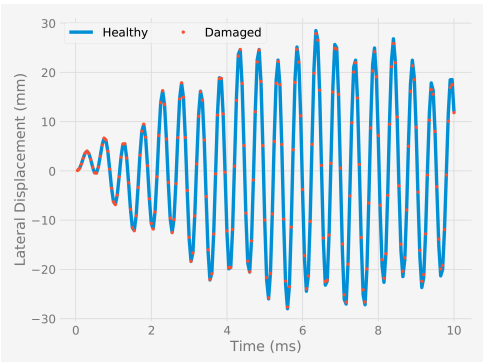

(e) $x = 63$ mm

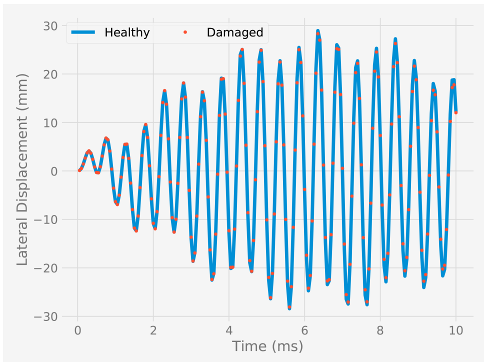

(f) $x = 66$ mm

FIGURE 2. The lateral displacements at the six observation points for the healthy and damaged conditions

TABLE 1. The first nine natural frequencies of the beam on the healthy and damaged conditions

Mode No.	Natural Frequency (kHz)		
	Healthy Condition	Damaged Condition	Change (%)
1	0.507	0.507	0.037
2	1.987	1.985	0.095
3	4.226	4.222	0.101
4	4.327	4.323	0.095
5	4.849	4.847	0.037
6	7.382	7.379	0.048
7	9.699	9.690	0.098
8	11.003	11.000	0.022
9	12.678	12.673	0.041

As for the damaged condition, the indicator computed at $x = 60$ mm is the most sensitive to the damage. The point is on the right end of the damaged segment. The sensitivity to the damage quickly drops by increasing the distance from the damaged element.

Finally, we discuss the damage indicator in the frequency domain. It is shown in Figure 3. Comparing with those in the time domain reveals some interesting differences and similarities. For the observation points at $x = 51$ mm and $x = 66$ mm, the indicator established in the time and frequency domains is not able to detect the damage. However, at the other measurement points where the effect of damage is detectable, the frequency domain representation is more distinctive and consistent. The indicator for the case of damage is clearly separated from the case of the healthy condition.

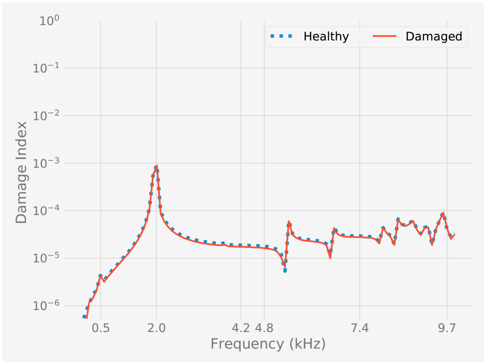

(a) $x = 51$ mm

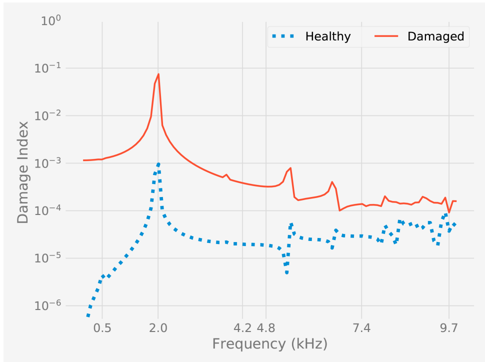

(b) $x = 54$ mm

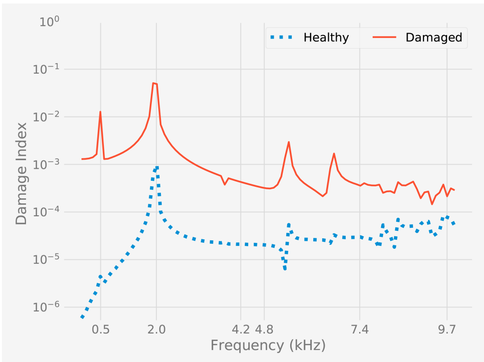

(c) $x = 57$ mm

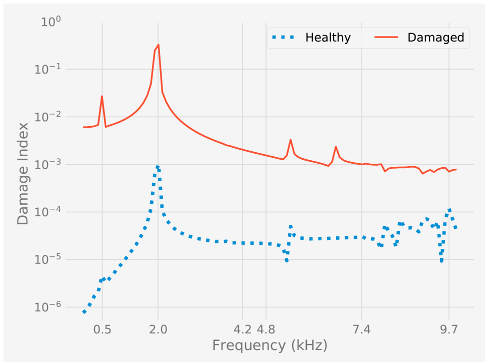

(d) $x = 60$ mm

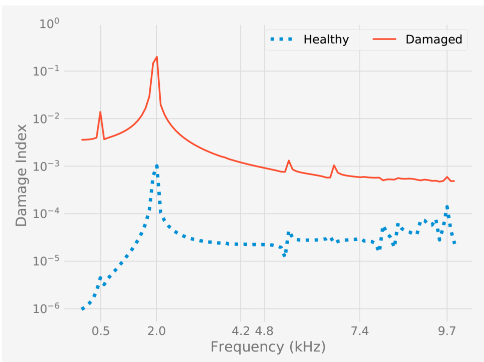

(e) $x = 63$ mm

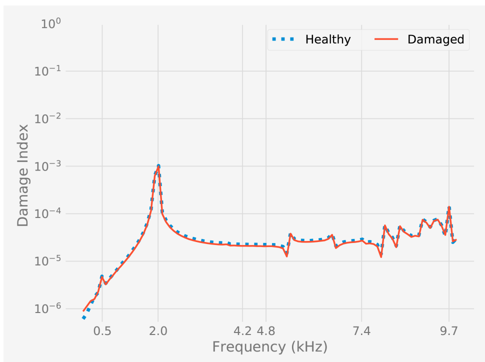

(f) $x = 66$ mm

FIGURE 3. The values of the damage indicator computed in the frequency domain

4. **Conclusion.** In this paper, we propose a damage indicator for assessing the change in structural condition. In general, the indicator is derived from our understanding of mechanics of materials and theory of elasticity. With those theories in mind, we understand and can predict the dynamical behavior of engineering structure upon receiving

external loads. The deviation of responses from our prediction may signify alteration of the structural integrity. We evaluate our theory with data collected from a vibration analysis of a simply supported beam. The vibration is simulated numerically by the finite element method. To simplify the issue, we alter the elastic modulus of a presumed damaged element by a small amount. We analyze the structural responses on the healthy and damaged conditions. Then, we compute the proposed damage indicator. We witness the sensitivity of the indicator to the altered element. We also evaluate the change of the natural frequencies due to the damaged element and witness that the change is too small for the frequencies to be affected. With that example, we conclude that the proposed indicator can potentially detect structural changes better than the traditional method based on the natural frequency.

So far, we have evaluated our damage indicator by using an idealized structure [31] and a simply-supported beam with a simple damage model, the current paper. Many studies are still required to evaluate the effectiveness of the method, including for the cases of breathing crack and delamination in composite structures. We will leave those issues for future works.

REFERENCES

[1] K. Zgonc and J. D. Achenbach, A neural network for crack sizing trained by finite element calculations, *NDT & E International*, vol.29, no.3, pp.147-155, 1996.

[2] J. R. Mohanty, B. B. Verma, D. R. K. Parhi and P. K. Ray, Application of artificial neural network for predicting fatigue crack propagation life of aluminum alloys, *Archives of Computational Materials Science and Surface Engineering*, vol.1, no.3, pp.133-138, 2009.

[3] D. Gope, P. C. Gope, A. Thakur and A. Yadav, Application of artificial neural network for predicting crack growth direction in multiple cracks geometry, *Applied Soft Computing*, vol.30, pp.514-528, 2015.

[4] M. M. Alamdari, T. Rakotoarivelo and N. L. D. Khoa, A spectral-based clustering for structural health monitoring of the sydney harbour bridge, *Mechanical Systems and Signal Processing*, vol.87, pp.384-400, 2017.

[5] S.-Y. Chu and S.-C. Lo, Application of real-time adaptive identification technique on damage detection and structural health monitoring, *Structural Control Health Monitoring*, vol.16, pp.154-177, 2009.

[6] E. Caetano, S. Silva and J. Bateira, A vision system for vibration monitoring of civil engineering, *Experimental Techniques*, vol.35, pp.74-82, 2011.

[7] J. M. W. Brownjohn, A. D. Stefano, Y.-L. Xu, H. Wenzel and A. E. Aktan, Vibration-based monitoring of civil infrastructure: Challenges and successes, *J. Civil Struct Health Monit.*, vol.1, pp.79-95, 2011.

[8] T. You, P. Li, Y. Chen and H. Ye, Structural health monitoring of bridge using an adaptive real-time wireless sensor network, *Journal of Convergence Information Technology*, vol.7, no.5, pp.28-35, 2012.

[9] L. Yu, J. H. Zhu and L. L. Yu, Structural damage detection in a truss bridge model using fuzzy clustering and measured FRF data reduced by principal component projection, *Advances in Structural Engineering*, vol.16, no.1, pp.207-217, 2013.

[10] P. Moser and B. Moaveni, Design and deployment of a continuous monitoring system for the downling hall footbridge, *Experimental Techniques*, vol.37, pp.15-26, 2013.

[11] A. Cigada, G. Moschioni, M. Vanali and A. Caprioli, The measurement network of the san siro meazza stadium in milan: Origin and implementation of a new data acquisition strategy for structural health monitoring, *Experimental Techniques*, vol.34, pp.70-81, 2009.

[12] C. Katsikeros and G. Labeas, Development and validation of a strain-based structural health monitoring system, *Mechanical Systems and Signal Processing*, vol.23, no.2, pp.372-383, http://www.sciencedirect.com/science/article/pii/S0888327008000721, 2009.

[13] A. Candelieri, R. Sormani, G. Arosio, I. Giordani and F. Archetti, Assessing structural health of helicopter fuselage panels through artificial neural networks hierarchies, *International Journal of Reliability and Safety*, vol.7, no.3, pp.216-234, 2013.

[14] A. Candelieri, R. Sormani, G. Arosio, I. Giordani and F. Archetti, A hyper-solution SVM classification framework: Application to on-line aircraft structural health monitoring, *Procedia-Social and Behavioral Sciences*, vol.108, pp.57-68, 2014.

[15] M. S. Mhaske and R. S. Shelke, Detection of crack location and depth in a cantilever beam vibration measurement and its comparative validation in ANN and GA, *International Journal of Research in Engineering and Technology*, vol.4, no.10, pp.152-157, 2015.

[16] F. Archetti, G. Arosio, A. Candelieri, I. Giordani and R. Sormani, Smart data driven maintenance: Improving damage detection and assessment on aerospace structures, *Metrology for Aerospace (MetroAeroSpace)*, IEEE, pp.101-106, 2014.

[17] W. Nick, J. Shelton, K. Asamene and E. Albert, A study of supervised machine learning techniques for structural health monitoring, *Proc. of the 26th Modern AI and Cognitive Science Conference*, Greensboro, NC, USA, pp.133-138, 2015.

[18] J. Mohanty, B. Verma, P. Ray and D. Parhi, Application of adaptive neuro-fuzzy inference system in modeling fatigue life under interspersed mixed-mode (i and ii) spike overload, *Expert Systems with Applications*, vol.38, no.10, pp.12 302-12 311, http://www.sciencedirect.com/science/article/pii/S0957417411005240, 2011.

[19] J. Mohanty, B. Verma, P. Ray and D. Parhi, Prediction of mode-i overload-induced fatigue crack growth rates using neuro-fuzzy approach, *Expert Systems with Applications*, vol.37, no.4, pp.3075-3087, http://www.sciencedirect.com/science/article/pii/S0957417409008033, 2010.

[20] M. Mehrjoo, N. Khaji, H. Moharrami and A. Bahreininejad, Damage detection of truss bridge joints using artificial neural networks, *Expert Systems with Applications*, vol.35, no.3, pp.1122-1131, 2008.

[21] F. dos Santos, B. Peeters, H. V. der Auweraer, L. Goes and W. Desmet, Vibration-based damage detection for a composite helicopter main rotorblade, *Mechanical Systems and Signal Processing*, vol.3, pp.22-27, 2016.

[22] R. de Medeiros, M. Sartorato, D. Vandepitte and V. Tita, A comparative assessment of different frequency based damage detection in unidirectional composite plates using MFC sensors, *Journal of Sound and Vibration*, vol.383, pp.171-190, 2016.

[23] M. M. Quinones, L. A. Montejo and S. Jang, Experimental and numerical evaluation of wavelet based damage detection methodologies, *Int. J. Adv. Struct. Eng.*, vol.7, pp.69-80, 2015.

[24] N. G. Pnevmatikos and G. D. Hatzigeorgiou, Damage detection of framed structures subjected to earthquake excitation using discrete wavelet analysis, *Bulletin of Earthquake Engineering*, vol.15, no.1, pp.227-248, 2017.

[25] M. Pedram, A. Esfandiari and M. R. Khedmati, Damage detection by a FE model updating method using power spectral density: Numerical and experimental investigation, *Journal of Sound and Vibration*, 2017.

[26] M. Cao, M. Radzieński, W. Xu and W. Ostachowicz, Identification of multiple damage in beams based on robust curvature mode shapes, *Mechanical Systems and Signal Processing*, vol.46, no.2, pp.468-480, 2014.

[27] E.-T. Lee and H.-C. Eun, Structural damage detection by power spectral density estimation using output-only measurement, *Shock and Vibration*, vol.2016, pp.2016-2022, 2016.

[28] D. D. Mandal, D. Wadadar and S. Banerjee, Performance evaluation of damage detection algorithms for identification of debond in stiffened metallic plates using a scanning laser vibrometer, *Journal of Vibration and Control*, p.1077546316687956, 2017.

[29] U. Baneen and Z. Kausar, A baseline-free modal strain energy method for damage localisation, *International Journal of Civil Engineering*, vol.10, pp.1-12, 2017.

[30] F. E. Gunawan, Reliability of the power spectral density method in predicting structural integrity, *International Journal of Innovative Computing, Information and Control*, vol.15, no.5, pp.1717-1727, http://www.ijicic.org/ijicic-150508.pdf, 2019.

[31] F. E. Gunawan, The sensitivity of the damage index of the general vibration method to damage level for structural health monitoring, *ICIC Express Letters*, vol.13, no.10, pp.931-939, http://www.icicel.org/ell/contents/2019/10/el-13-10-08.pdf, 2019.

[32] J. F. Doyle, *Wave Propagation in Structures: An FFT-Based Spectral Analysis Methodology*, Springer-Verlag, New York, 1989.